



This is a repository copy of *Efficient Two-Dimensional Direction-of-Arrival Estimation for a Mixture of Circular and Noncircular Sources*.

White Rose Research Online URL for this paper:  
<http://eprints.whiterose.ac.uk/99229/>

Version: Accepted Version

---

**Article:**

Chen, H., Hou, C., Liu, W. [orcid.org/0000-0003-2968-2888](https://orcid.org/0000-0003-2968-2888) et al. (2 more authors) (2016) Efficient Two-Dimensional Direction-of-Arrival Estimation for a Mixture of Circular and Noncircular Sources. *IEEE Sensors Journal*, 16 (8). pp. 2527-2536. ISSN 1530-437X

<https://doi.org/10.1109/JSEN.2016.2517128>

---

© 2016 IEEE. Personal use of this material is permitted. Permission from IEEE must be obtained for all other users, including reprinting/ republishing this material for advertising or promotional purposes, creating new collective works for resale or redistribution to servers or lists, or reuse of any copyrighted components of this work in other works.

**Reuse**

Unless indicated otherwise, fulltext items are protected by copyright with all rights reserved. The copyright exception in section 29 of the Copyright, Designs and Patents Act 1988 allows the making of a single copy solely for the purpose of non-commercial research or private study within the limits of fair dealing. The publisher or other rights-holder may allow further reproduction and re-use of this version - refer to the White Rose Research Online record for this item. Where records identify the publisher as the copyright holder, users can verify any specific terms of use on the publisher's website.

**Takedown**

If you consider content in White Rose Research Online to be in breach of UK law, please notify us by emailing [eprints@whiterose.ac.uk](mailto:eprints@whiterose.ac.uk) including the URL of the record and the reason for the withdrawal request.



[eprints@whiterose.ac.uk](mailto:eprints@whiterose.ac.uk)  
<https://eprints.whiterose.ac.uk/>

# Efficient Two-Dimensional Direction of Arrival Estimation for a Mixture of Circular and Noncircular Sources

Hua Chen, Chunping Hou, Wei Liu, *Senior Member, IEEE*, Wei-Ping Zhu, *Senior Member, IEEE* and M.N.S. Swamy, *Fellow, IEEE*

**Abstract**—In this paper, the two-dimensional (2-D) direction-of-arrival (DOA) estimation problem for a mixture of circular and non-circular sources is considered. In particular, we focus on a 2-D array structure consisting of two parallel uniform linear arrays (ULAs) and build a general array model with mixed circular and non-circular sources. The received array data and its conjugate counterparts are combined together to form a new data vector, based on which a series of 2-D DOA estimators are derived. Compared to existing methods, the proposed one has three main advantages. Firstly, it can give a more accurate estimation in situations where the number of sources is within the traditional limit of high resolution methods; secondly, it can still work effectively when the number of mixed signals is larger than that of the array elements; thirdly, the paired 2-D DOAs of the proposed method can be obtained automatically without the complicated 2-D spectrum peak search and therefore has a much lower computational complexity.

**Index Terms**—Two-dimensional (2-D), Direction of arrival (DOA), non-circular signal, rank-reduction, planar arrays

## I. INTRODUCTION

THE estimation of two-dimensional (2-D) direction of arrival (DOA) is an important area of array signal processing and has received much attention in past years [1, 2]. Many effective methods and algorithms have been proposed based on different array structures, such as two-parallel uniform linear arrays (ULAs) [3–7], L-shaped ULAs [8–13], and uniform rectangular arrays (URAs) [14–16].

In most traditional DOA estimation algorithms, only the traditional covariance matrix is considered which characterizes the circular Gaussian distribution and in recent years, the DOA estimation problem for non-circular signals has attracted more and more attention, first for one-dimensional (1-D) or linear arrays [17–25], and then extended to the 2-D case [26–28]. By exploiting this additional noncircularity information, an improved performance can be achieved for both 1-D and 2-D DOA estimation. In particular, in [26], Liu. et al proposed an ERARE method for noncircular sources based on two-parallel ULAs, with improved estimation accuracy compared

to [4]; based on [13], the estimation accuracy was also improved with the conjugate information of the observed data for L-shaped ULAs in [27]. By employing non-circular signal constellations, Roemer and Haardt proposed a DOA estimation algorithm for a regular-hexagonal shaped ESPAR array, with a detailed analysis of the Cramer-Rao bound (CRB) [28].

A more general problem is that the impinging signals to the array are a mixture of circular and non-circular ones, such as a mixture of quadrature phase shift keying (QPSK) signals (circular) and binary phase shift keying (BPSK) signals (non-circular). This problem has been studied for DOA estimation of 1-D arrays and several approaches have been proposed [29–31]. In [29], a new data vector was formed by combining the original data and its conjugate version to construct two estimators for direction finding of circular and non-circular signals, respectively. However, it can not deal with the problem when the DOAs of the circular and non-circular signals are coincident, and a small angle separation between them will lead to severe performance degradation. An improved algorithm was then proposed in [30], which estimates the DOAs of circular and non-circular signals separately by exploiting the difference between the circularity properties of the signals. Nevertheless, when the number of data samples is small, its DOA estimation performance will degrade. In [31], the problem was solved using a sparse representation algorithm, which employs overcomplete dictionaries subject to sparsity constraints to jointly represent the covariance and elliptic covariance matrices of the array output. However, to our best knowledge, the 2-D DOA estimation problem for mixed circular and non-circular impinging signals has not yet been addressed in literature.

In this paper, we fill this gap and study the problem based on the 2-D structure consisting of two parallel ULAs. Starting from the non-circular signal only formulations in [26], we first build a general array model to accommodate the case with mixed circular and non-circular signals and then propose a novel method for 2-D DOA estimation. One advantage of the proposed method is that it can give a more accurate estimation in situations where the number of sources is within the traditional limit of high resolution methods in [3]; secondly, it can still work effectively when the number of mixed signals is larger than that of the array elements; thirdly, the paired 2-D DOAs of the proposed method can be obtained automatically without the complicated 2-D spectrum peak search. Extensive simulation results will be provided to show the performance

This work is supported by the National 863 Programs under Grant (No. 2015AA01A706) and China Scholarship Council (CSC).

Hua Chen, Chunping Hou are with the School of Electronic Information Engineering, Tianjin University, China, 300072. (e-mail: dkchenhua@tju.edu.cn.)

Wei Liu is with the Department of Electronic and Electrical Engineering, University of Sheffield, Sheffield S1 3JD, UK. (e-mail: w.liu@sheffield.ac.uk).

Wei-Ping Zhu and M.N.S. Swamy are with the Department of Electrical and Computer Engineering, Concordia University, Montreal, QC H3G 1M8, Canada. (e-mail: weiping@ece.concordia.ca; swamy@ece.concordia.ca).

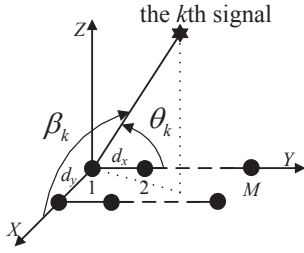


Fig. 1. Geometry of the array model.

of our proposed method.

Throughout the paper,  $(\cdot)^*$ ,  $(\cdot)^T$ ,  $(\cdot)^{-1}$  and  $(\cdot)^H$  represent conjugation, transpose, inverse and conjugate transpose, respectively.  $E(\cdot)$  is the expectation operation;  $\text{diag}(\cdot)$  stands for the diagonalization operation;  $\mathbf{I}_p$  denotes the  $p \times p$  dimensional identity matrix;  $\det[\cdot]$  is the determinant of a matrix.

## II. PROBLEM FORMULATION

As shown in Fig.1, suppose that there are  $K = K_n + K_c$  uncorrelated far-field sources impinging upon the array with  $K_n$  noncircular sources  $s_{n,k}(t)$  and  $K_c$  circular sources  $s_{c,k}(t)$ , from directions  $(\theta_k, \beta_k)$ ,  $k = 1, 2, \dots, K$ . The array consists of two parallel ULAs with each one having  $M$  elements. The distance between the two ULAs is  $\lambda/2$ , denoted as  $d_y$ , and the inter-element spacing  $d_x$  for each ULA is also  $\lambda/2$ , where  $\lambda$  is the wavelength of the incident waves. The additive noises of the two ULAs are circular Gaussian with zero mean and variance  $\sigma^2$ , which are uncorrelated with the impinging signals. The output data vectors  $\mathbf{x}(t) = [x_1(t), x_2(t), \dots, x_M(t)]$  and  $\mathbf{y}(t) = [y_1(t), y_2(t), \dots, y_M(t)]$  of the two ULAs at sample  $t$  can be modeled as

$$\mathbf{x}(t) = \mathbf{A}\tilde{\mathbf{s}}(t) + \mathbf{n}_x(t) \quad (1)$$

$$\mathbf{y}(t) = \mathbf{A}\tilde{\mathbf{B}}\tilde{\mathbf{s}}(t) + \mathbf{n}_y(t) \quad (2)$$

where  $\mathbf{A}$  is the steering matrix with each column denoted by  $\mathbf{a}(\theta_k)$ , given by  $\mathbf{a}(\theta_k) = [a_0(\theta_k), \dots, a_{M-1}(\theta_k)]^T$  with  $a_i(\theta_k) = e^{-j\frac{2\pi}{\lambda}d_x(i)\cos\theta_k}$ ,  $\mathbf{B}(\beta)$  is termed as the steering element matrix given by  $\mathbf{B} = \text{diag}[v(\beta_1), v(\beta_2), \dots, v(\beta_K)]$ , with  $v(\beta_k) = e^{j\frac{2\pi}{\lambda}d_y\cos\beta_k}$ ,  $\mathbf{n}_x(t) = [n_{x,1}(t), \dots, n_{x,M}(t)]^T$  and  $\mathbf{n}_y(t) = [n_{y,1}(t), \dots, n_{y,M}(t)]^T$  represent the circular Gaussian noise vectors of the two arrays, respectively, and  $\tilde{\mathbf{s}}(t) = [s_{n,1}(t), \dots, s_{n,K_n}(t), s_{c,1}(t), \dots, s_{c,K_c}(t)]^T$  is the mixed source signal vector which has the following form

$$\tilde{\mathbf{s}}(t) = \dot{\mathbf{B}}\mathbf{s}(t) \quad (3)$$

In (3),  $\dot{\mathbf{B}}$  is given by

$$\begin{aligned} \dot{\mathbf{B}} &= \text{diag} \left[ b_{n,1}, \dots, b_{n,K_n}, \underbrace{1, \dots, 1}_{K_c} \right] \\ &= \begin{bmatrix} \dot{\mathbf{B}}_1 & \mathbf{0} \\ \mathbf{0} & \dot{\mathbf{B}}_2 \end{bmatrix} \end{aligned} \quad (4)$$

where  $\dot{\mathbf{B}}_1 = \text{diag}[b_{n,1}, \dots, b_{n,K_n}]$ ,  $\dot{\mathbf{B}}_2 = \mathbf{I}_{K_c}$ , and  $\mathbf{s}(t)$  is defined as

$$\mathbf{s}(t) = [\bar{s}_{n,1}(t), \dots, \bar{s}_{n,K_n}(t), s_{c,1}(t), \dots, s_{c,K_c}(t)]^T. \quad (5)$$

We assume  $s_{n,k}(t)$  is a strictly noncircular (rectilinear) signal [32, 33]. Then it can be expressed as  $s_{n,k}(t) = b_{n,k}\bar{s}_{n,k}(t)$ , where  $\bar{s}_{n,k}(t)$  is a real signal, and  $b_{n,k} = e^{j\varphi_k}$  ( $k = 1, \dots, K_n$ ) is an arbitrary phase shift for the signal.

## III. THE PROPOSED METHOD

In this section, the 2-D DOA estimation algorithm for a general mixture of circular and non-circular signals impinging on the two parallel ULAs is derived in detail, based on the observed data coupled with its conjugate counterparts.

### A. General array model

By concatenating the observed data vectors  $\mathbf{x}(t)$  and  $\mathbf{y}(t)$ , we define a new data vector  $\mathbf{z}(t)$  as follows

$$\begin{aligned} \mathbf{z}(t) &= \begin{bmatrix} \mathbf{x}(t) \\ \mathbf{y}(t) \end{bmatrix} = \begin{bmatrix} \mathbf{A}(\theta) \\ \mathbf{A}(\theta)\mathbf{B}(\beta) \end{bmatrix} \dot{\mathbf{B}}\mathbf{s}(t) + \begin{bmatrix} \mathbf{n}_x(t) \\ \mathbf{n}_y(t) \end{bmatrix} \\ &= \mathbf{C}(\theta, \beta)\dot{\mathbf{B}}\mathbf{s}(t) + \mathbf{n}(t). \end{aligned} \quad (6)$$

For simplified notation, the pair of angles  $(\theta, \beta)$  together with  $t$  are omitted in the following when not causing any confusion.

In (6),  $\mathbf{C}(\theta, \beta)$  is named as the extended steering vector with each column denoted as  $\mathbf{c}(\theta, \beta)$ , which can be expressed as

$$\mathbf{C} = [\mathbf{C}_1(\theta_n, \beta_n) \quad \mathbf{C}_2(\theta_c, \beta_c)] \quad (7)$$

where

$$\begin{aligned} \mathbf{C}_1 &= \begin{bmatrix} \mathbf{a}(\theta_{n,1}) & \dots & \mathbf{a}(\theta_{n,K_n}) \\ \mathbf{a}(\theta_{n,1})v(\beta_{n,1}) & \dots & \mathbf{a}(\theta_{n,K_n})v(\beta_{n,K_n}) \end{bmatrix} \\ &= \begin{bmatrix} \mathbf{a}_{n,1} & \dots & \mathbf{a}_{n,K_n} \\ \mathbf{a}_{n,1}v_{n,1} & \dots & \mathbf{a}_{n,K_n}v_{n,K_n} \end{bmatrix} \end{aligned} \quad (8)$$

$$\begin{aligned} \mathbf{C}_2 &= \begin{bmatrix} \mathbf{a}(\theta_{c,1}) & \dots & \mathbf{a}(\theta_{c,K_c}) \\ \mathbf{a}(\theta_{c,1})v(\beta_{c,1}) & \dots & \mathbf{a}(\theta_{c,K_c})v(\beta_{c,K_c}) \end{bmatrix} \\ &= \begin{bmatrix} \mathbf{a}_{c,1} & \dots & \mathbf{a}_{c,K_c} \\ \mathbf{a}_{c,1}v_{c,1} & \dots & \mathbf{a}_{c,K_c}v_{c,K_c} \end{bmatrix} \end{aligned} \quad (9)$$

are  $2M \times K_n$  and  $2M \times K_c$  matrices, respectively.

Then, another new data vector  $\check{\mathbf{z}}$  is defined by combining the vector  $\mathbf{z}$  and its conjugate counterpart  $\mathbf{z}^*$  as follows

$$\check{\mathbf{z}} = \begin{bmatrix} \mathbf{z} \\ \mathbf{z}^* \end{bmatrix} = \begin{bmatrix} \mathbf{C}\dot{\mathbf{B}}\mathbf{s} \\ \mathbf{C}^*\dot{\mathbf{B}}^*\mathbf{s}^* \end{bmatrix} + \begin{bmatrix} \mathbf{n} \\ \mathbf{n}^* \end{bmatrix} = \check{\mathbf{C}}\check{\mathbf{s}} + \check{\mathbf{n}} \quad (10)$$

where  $\check{\mathbf{C}}$  is a  $4M \times (K_n + 2K_c)$  matrix, i.e.,

$$\check{\mathbf{C}} = [\check{\mathbf{c}}_{n,1}, \dots, \check{\mathbf{c}}_{n,K_n}, \check{\mathbf{c}}_{c,1}, \dots, \check{\mathbf{c}}_{c,K_c}] \quad (11)$$

with

$$\check{\mathbf{c}}_{n,k} = \begin{bmatrix} b_{n,k} \begin{pmatrix} \mathbf{a}_{n,k} \\ \mathbf{a}_{n,k}v_{n,k} \end{pmatrix} \\ b_{n,k}^* \begin{pmatrix} \mathbf{a}_{n,k}^* \\ \mathbf{a}_{n,k}^*v_{n,k}^* \end{pmatrix} \end{bmatrix} \quad (12)$$

being a  $4M \times 1$  vector ( $k = 1, 2, \dots, K_n$ ), and

$$\check{\mathbf{c}}_{c,k} = \begin{bmatrix} \mathbf{a}_{c,k} & \mathbf{0}_{M \times 1} \\ \mathbf{a}_{c,k}v_{c,k} & \mathbf{0}_{M \times 1} \\ \mathbf{0}_{M \times 1} & \mathbf{a}_{c,k}^* \\ \mathbf{0}_{M \times 1} & \mathbf{a}_{c,k}^*v_{c,k}^* \end{bmatrix} \quad (13)$$

being a  $4M \times 2$  matrix ( $k = 1, 2, \dots, K_c$ ),

$$\check{\mathbf{s}} = [s_{n,1}, \dots, s_{n,K_n}, s_{c,1}, s_{c,1}^*, \dots, s_{c,K_c}, s_{c,K_c}^*]^T \quad (14)$$

is a  $(K_n + 2K_c) \times 1$  vector, and

$$\check{\mathbf{n}} = \begin{bmatrix} \mathbf{n} \\ \mathbf{n}^* \end{bmatrix} \quad (15)$$

is a  $4M \times 1$  vector.

Based on the above general array model, the proposed method is derived in the following section.

### B. Main method

The covariance matrix of  $\check{\mathbf{z}}$  is given by

$$\check{\mathbf{R}} = E[\check{\mathbf{z}}\check{\mathbf{z}}^H] = \check{\mathbf{C}}\mathbf{R}_s\check{\mathbf{C}}^H + \sigma^2\mathbf{I}_{4M} \quad (16)$$

where  $\check{\mathbf{R}}_s = E[\check{\mathbf{s}}\check{\mathbf{s}}^H]$  is the covariance matrix of  $\check{\mathbf{s}}$ .

**Remark 1:** In practice, only a finite number of observed data is available. Thus,  $\check{\mathbf{R}}$  is estimated by

$$\check{\mathbf{R}} \approx \frac{1}{L} \sum_{l=1}^L \check{\mathbf{z}}(l)\check{\mathbf{z}}^H(l), \quad (17)$$

where  $L$  denotes the number of snapshots. With less observed data, there will be a larger error in the estimated covariance matrix, which will lead to a degradation in performance.

Since the signals are not correlated with each other,  $\check{\mathbf{R}}_s$  is a full rank matrix. Then the eigen-value decomposition (EVD) of  $\check{\mathbf{R}}$  is

$$\check{\mathbf{R}} = \mathbf{E}_s\mathbf{\Sigma}_s\mathbf{E}_s^H + \mathbf{E}_n\mathbf{\Sigma}_n\mathbf{E}_n^H \quad (18)$$

where the  $4M \times (K_n + 2K_c)$  matrix  $\mathbf{E}_s$  and the  $4M \times (4M - K_n - 2K_c)$  matrix  $\mathbf{E}_n$  are the signal subspace and noise subspace, respectively. The  $(K_n + 2K_c) \times (K_n + 2K_c)$  matrix  $\mathbf{\Sigma}_s = \text{diag}(\lambda_1, \lambda_2, \dots, \lambda_K)$  and the  $(4M - K_n - 2K_c) \times (4M - K_n - 2K_c)$  matrix  $\mathbf{\Sigma}_n = \text{diag}(\lambda_{K+1}, \lambda_{K+2}, \dots, \lambda_{4M})$  are the corresponding diagonal matrices, where  $\lambda_1 \geq \lambda_2 \geq \dots \geq \lambda_K > \lambda_{K+1} = \dots = \lambda_{4M} = \sigma^2$  are the eigenvalues of  $\check{\mathbf{R}}$ .

Considering that both  $\check{\mathbf{C}}$  and  $\mathbf{E}_s$  span the signal subspace, which are orthogonal to the noise subspace spanned by the matrix  $\mathbf{E}_n$ , we derive the following estimators to obtain the 2-D DOAs of noncircular and circular signals using the rank-reduction method.

1) *2-D DOA estimation for noncircular sources:* Based on the orthogonality between  $\mathbf{E}_n$  and  $\check{\mathbf{c}}_{n,k}$ , the following equation holds for any direction from  $(\theta_{n,k}, \beta_{n,k})$

$$\mathbf{E}_n^H \check{\mathbf{c}}_{n,k} = \mathbf{0} \quad (19)$$

In order to avoid the 2-D spectrum peak search related to  $(\theta_{n,k}, \beta_{n,k})$  in a grid area, together with (13), (19) can be

rewritten as

$$\begin{aligned} & \mathbf{0} \\ &= \mathbf{E}_n^H \check{\mathbf{c}}_{n,k} \\ &= \mathbf{E}_n^H \begin{bmatrix} b_{n,k} \begin{pmatrix} \mathbf{a}_{n,k} \\ \mathbf{a}_{n,k} v_{n,k} \end{pmatrix} \\ b_{n,k}^* \begin{pmatrix} \mathbf{a}_{n,k}^* \\ \mathbf{a}_{n,k}^* v_{n,k}^* \end{pmatrix} \end{bmatrix} \\ &= \mathbf{E}_n^H \begin{bmatrix} b_{n,k} \begin{pmatrix} \mathbf{a}_{n,k} & \mathbf{0}_{M \times 1} \\ \mathbf{0}_{M \times 1} & \mathbf{a}_{n,k} \end{pmatrix} \begin{pmatrix} 1 \\ v_{n,k} \end{pmatrix} \\ b_{n,k}^* \begin{pmatrix} \mathbf{a}_{n,k}^* & \mathbf{0}_{M \times 1} \\ \mathbf{0}_{M \times 1} & \mathbf{a}_{n,k}^* \end{pmatrix} \begin{pmatrix} 1 \\ v_{n,k}^* \end{pmatrix} \end{bmatrix} \\ &= \mathbf{E}_n^H \begin{bmatrix} \mathbf{a}_{n,k} & & & \\ & \mathbf{a}_{n,k} & & \\ & & \mathbf{a}_{n,k}^* & \\ & & & \mathbf{a}_{n,k}^* \end{bmatrix} \begin{bmatrix} b_{n,k} \\ b_{n,k} v_{n,k} \\ b_{n,k}^* \\ b_{n,k}^* v_{n,k}^* \end{bmatrix} \\ &= \mathbf{E}_n^H \begin{bmatrix} \mathbf{a}_{n,k} & & & \\ & \mathbf{a}_{n,k} & & \\ & & \mathbf{a}_{n,k}^* & \\ & & & \mathbf{a}_{n,k}^* \end{bmatrix} \begin{bmatrix} 1 & 0 \\ v_{n,k} & 0 \\ 0 & 1 \\ 0 & v_{n,k}^* \end{bmatrix} \begin{bmatrix} b_{n,k} \\ b_{n,k}^* \end{bmatrix} \end{aligned} \quad (20)$$

Defining a  $4M \times 4$  matrix  $\mathbf{\Omega}(\theta)$  which is only related to  $\theta$

$$\mathbf{\Omega}(\theta) = \begin{bmatrix} \mathbf{a}(\theta) & & & \\ & \mathbf{a}(\theta) & & \\ & & \mathbf{a}^*(\theta) & \\ & & & \mathbf{a}^*(\theta) \end{bmatrix} \quad (21)$$

and

$$\mathbf{p}_n(\theta) = \mathbf{\Omega}^H(\theta)\mathbf{E}_n\mathbf{E}_n^H\mathbf{\Omega}(\theta) \quad (22)$$

we obtain the following estimator over  $\theta$  corresponding to noncircular signals as

$$f_n(\theta) = [\det(\mathbf{p}_n(\theta))]^{-1} = [\det(\mathbf{\Omega}^H(\theta)\mathbf{E}_n\mathbf{E}_n^H\mathbf{\Omega}(\theta))]^{-1} \quad (23)$$

If searched over the confined region with  $\theta \in [0, \pi]$ , the DOAs  $\theta_{n,k}$  of noncircular sources can be obtained from peaks in  $f_n$ .

We then substitute the estimated  $\theta$  of noncircular sources into (20) and have the following estimator over  $\beta$  corresponding to noncircular signals

$$f'_n(\beta) = [\det(\mathbf{p}'_n(\beta))]^{-1} \quad (24)$$

where

$$\mathbf{p}'_n(\beta) = \mathbf{\Theta}^H(\beta)\mathbf{\Omega}^H(\theta)\mathbf{E}_n\mathbf{E}_n^H\mathbf{\Omega}(\theta)\mathbf{\Theta}(\beta) \quad (25)$$

and

$$\mathbf{\Theta}(\beta) = \begin{bmatrix} 1 & 0 \\ v(\beta) & 0 \\ 0 & 1 \\ 0 & v^*(\beta) \end{bmatrix} \quad (26)$$

2) *2-D DOA estimation for circular sources:* The orthogonality between  $\mathbf{E}_n$  and  $\check{\mathbf{C}}_{c,k}$  still holds, i.e.

$$\mathbf{E}_n^H \check{\mathbf{C}}_{c,k} = \mathbf{E}_n^H \begin{bmatrix} \mathbf{a}_{c,k} & \mathbf{0}_{M \times 1} \\ \mathbf{a}_{c,k} v_{c,k} & \mathbf{0}_{M \times 1} \\ \mathbf{0}_{M \times 1} & \mathbf{a}_{c,k}^* \\ \mathbf{0}_{M \times 1} & \mathbf{a}_{c,k}^* v_{c,k}^* \end{bmatrix} = \mathbf{0}. \quad (27)$$

From (27), we have

$$\mathbf{E}_n^H \begin{bmatrix} \mathbf{a}_{c,k} \\ \mathbf{a}_{c,k}v_{c,k} \\ \mathbf{0}_{M \times 1} \\ \mathbf{0}_{M \times 1} \end{bmatrix} = \mathbf{0} \quad (28)$$

and

$$\mathbf{E}_n^H \begin{bmatrix} \mathbf{0}_{M \times 1} \\ \mathbf{0}_{M \times 1} \\ \mathbf{a}_{c,k}^* \\ \mathbf{a}_{c,k}^*v_{c,k}^* \end{bmatrix} = \mathbf{0} \quad (29)$$

Partitioning the matrix  $\mathbf{E}_n$  into  $\mathbf{E}_n = [\mathbf{E}_{n1}^T, \mathbf{E}_{n2}^T]^T$ , where  $\mathbf{E}_{n1}$  and  $\mathbf{E}_{n2}$  are two submatrices of the same size  $2M \times (4M - K_n - 2K_c)$ , (28) and (29) can be changed to

$$\begin{aligned} & \mathbf{0} \\ &= \begin{bmatrix} \mathbf{a}_{c,k} \\ \mathbf{a}_{c,k}v_{c,k} \\ 1 \\ v_{c,k} \end{bmatrix}^H \mathbf{E}_{n1} \mathbf{E}_{n1}^H \begin{bmatrix} \mathbf{a}_{c,k} \\ \mathbf{a}_{c,k}v_{c,k} \\ \mathbf{a}_{c,k} \\ \mathbf{a}_{c,k} \end{bmatrix} \\ &= \begin{bmatrix} 1 \\ v_{c,k} \end{bmatrix}^H \begin{bmatrix} \mathbf{a}_{c,k} \\ \mathbf{a}_{c,k} \end{bmatrix} \mathbf{E}_{n1} \mathbf{E}_{n1}^H \begin{bmatrix} \mathbf{a}_{c,k} \\ \mathbf{a}_{c,k} \end{bmatrix} \begin{bmatrix} 1 \\ v_{c,k} \end{bmatrix} \end{aligned} \quad (30)$$

and

$$\begin{aligned} & \mathbf{0} = \left[ \begin{pmatrix} \mathbf{a}_{c,k} \\ \mathbf{a}_{c,k}v_{c,k} \end{pmatrix}^* \right]^H (\mathbf{E}_{n2} \mathbf{E}_{n2}^H) \left[ \begin{pmatrix} \mathbf{a}_{c,k} \\ \mathbf{a}_{c,k}v_{c,k} \end{pmatrix} \right] \\ \Rightarrow & \mathbf{0} = \begin{bmatrix} \mathbf{a}_{c,k} \\ \mathbf{a}_{c,k}v_{c,k} \end{bmatrix}^H \mathbf{E}_{n2}^* (\mathbf{E}_{n2}^*)^H \begin{bmatrix} \mathbf{a}_{c,k} \\ \mathbf{a}_{c,k}v_{c,k} \end{bmatrix} \\ \Rightarrow & \mathbf{0} \\ &= \begin{bmatrix} \mathbf{a}_{c,k} \\ \mathbf{a}_{c,k}v_{c,k} \\ 1 \\ v_{c,k} \end{bmatrix}^H (\mathbf{E}_{n2} \mathbf{E}_{n2}^H)^* \begin{bmatrix} \mathbf{a}_{c,k} \\ \mathbf{a}_{c,k}v_{c,k} \\ \mathbf{a}_{c,k} \\ \mathbf{a}_{c,k} \end{bmatrix} \\ &= \begin{bmatrix} 1 \\ v_{c,k} \end{bmatrix}^H \begin{bmatrix} \mathbf{a}_{c,k} \\ \mathbf{a}_{c,k} \end{bmatrix} (\mathbf{E}_{n2} \mathbf{E}_{n2}^H)^* \\ & \times \begin{bmatrix} \mathbf{a}_{c,k} \\ \mathbf{a}_{c,k} \end{bmatrix} \begin{bmatrix} 1 \\ v_{c,k} \end{bmatrix} \end{aligned} \quad (31)$$

As shown in Appendix, (30) and (31) are equivalent to each other.

Here, based on (30), the estimator over  $\theta$  corresponding to circular signals is as follows.

Since

$$\begin{bmatrix} 1 \\ v_{c,k} \end{bmatrix} \neq \mathbf{0} \quad (32)$$

we have

$$f_c(\theta) = [\det(\mathbf{p}_c(\theta))]^{-1} \quad (33)$$

where

$$\mathbf{p}_c(\theta) = \mathbf{\Lambda}^H(\theta) \mathbf{E}_{n1} \mathbf{E}_{n1}^H \mathbf{\Lambda}(\theta) \quad (34)$$

and

$$\mathbf{\Lambda}(\theta) = \begin{bmatrix} \mathbf{a}_{c,k} & \\ & \mathbf{a}_{c,k} \end{bmatrix} \quad (35)$$

Similarly, the DOAs  $\theta_{c,k}$  of circular sources can be obtained from peaks in  $f_c$  by searching over the confined region only related to  $\theta$ .

With the estimated  $\theta$  of circular sources, we substitute them into (30) and have the following estimator over  $\beta$  corresponding to circular signals

$$f'_c(\beta) = (p'_c(\beta))^{-1} \quad (36)$$

where

$$p'_c(\beta) = \begin{bmatrix} \mathbf{a}(\theta) \\ \mathbf{a}(\theta)v(\beta) \end{bmatrix}^H \mathbf{E}_{n1} \mathbf{E}_{n1}^H \begin{bmatrix} \mathbf{a}(\theta) \\ \mathbf{a}(\theta)v(\beta) \end{bmatrix} \quad (37)$$

Note that the estimator in (33) is quite similar to the one in (23) except that  $\mathbf{E}_{n1}$ , half of the noise subspace matrix  $\mathbf{E}_n$ , is used in (33). However, the way to achieve  $\beta$  of noncircular and circular signals is different. The estimator in (24) uses the rank-reduction MUSIC method, while the estimator (36) uses the conventional MUSIC method.

### C. Circular and Noncircular Signals Identification

In order to discriminate the 2-D DOAs of circular signals from that of noncircular signals, we consider equation (27) again,

$$\begin{aligned} \mathbf{0} &= \mathbf{E}_n^H \check{\mathbf{C}}_{c,k} \\ &= \mathbf{E}_n^H \begin{bmatrix} \mathbf{a}_{c,k} & \mathbf{0}_{M \times 1} \\ \mathbf{a}_{c,k}v_{c,k} & \mathbf{0}_{M \times 1} \\ \mathbf{0}_{M \times 1} & \mathbf{a}_{c,k}^* \\ \mathbf{0}_{M \times 1} & \mathbf{a}_{c,k}^*v_{c,k}^* \end{bmatrix} \\ &= \mathbf{E}_n^H \begin{bmatrix} \mathbf{a}_{c,k} & & & \\ & \mathbf{a}_{c,k} & & \\ & & \mathbf{a}_{c,k}^* & \\ & & & \mathbf{a}_{c,k}^* \end{bmatrix} \begin{bmatrix} 1 \\ v_{c,k} \\ & 1 \\ & & 1 \\ & & & v_{c,k}^* \end{bmatrix} \end{aligned} \quad (38)$$

Due to  $\begin{bmatrix} 1 \\ v_{c,k} \\ & 1 \\ & & v_{c,k}^* \end{bmatrix} \neq \mathbf{0}$ , the following equations hold for circular signals too

$$[\det(\mathbf{\Omega}^H(\theta_{c,k}) \mathbf{E}_n \mathbf{E}_n^H \mathbf{\Omega}(\theta_{c,k}))^{-1} = 0 \quad (39)$$

and

$$[\det(\mathbf{\Theta}^H(\beta_{c,k}) \mathbf{\Omega}^H(\theta_{c,k}) \mathbf{E}_n \mathbf{E}_n^H \mathbf{\Omega}(\theta_{c,k}) \mathbf{\Theta}(\beta_{c,k}))^{-1} = 0. \quad (40)$$

It is concluded that the 2-D DOAs of both noncircular and circular signals can be obtained from (23) and (24), while the estimators (33) and (36) only identify the 2-D DOAs of circular signals. Therefore, the identification of circular and noncircular incident signals from their mixtures can be achieved.

### D. Summary of the proposed algorithm

The proposed algorithm is summarized as follows:

- 1) Calculate the covariance matrix  $\bar{\mathbf{R}}$  from the collected data.
- 2) Obtain the noise subspace  $\bar{\mathbf{E}}_n$  by performing EVD to  $\bar{\mathbf{R}}$ .
- 3) Use (23) and (24) to estimate the  $K$  2-D DOAs of the mixed signals.
- 4) Obtain  $\bar{\mathbf{E}}_{n1}$  by partitioning the matrix  $\bar{\mathbf{E}}_n$ .
- 5) Use (33) and (36) to estimate the  $K_c$  2-D DOAs of the circular signals.
- 6) Compare the spatial spectrum achieved by 3) and 5) to identify the  $K_n$  2-D DOAs of the noncircular signals.

**Remark 2:** Now we give a complexity analysis in terms of the number of complex-valued multiplications of the proposed method including the construction of  $\check{\mathbf{R}}$ , performing EVD of  $\check{\mathbf{R}}$  and spectral searching. To calculate  $\check{\mathbf{R}}$ , a computational complexity of  $O((4M)^2L)$  is needed. Define the scanning interval of  $\theta \in [0, \pi]$  with a stepsize  $\Delta\theta$ , and  $\beta \in [0, \pi]$  with a stepsize  $\Delta\beta$ , respectively. The proposed method employs several 1-D spatial spectrum search procedures to obtain the 2-D DOAs of noncircular and circular signals, which has a computational complexity of  $O\left(\frac{\pi}{\Delta\theta}(4M)^2 + K\frac{\pi}{\Delta\beta}(4M)^2 + \frac{\pi}{\Delta\theta}(2M)^2 + K_c\frac{\pi}{\Delta\beta}(2M)^2\right)$ , while two direct 2-D spatial spectrum search procedures entail a computational complexity of  $O\left(\frac{\pi}{\Delta\theta}\frac{\pi}{\Delta\beta}(4M)^2 + \frac{\pi}{\Delta\theta}\frac{\pi}{\Delta\beta}(2M)^2\right)$ .

**Remark 3:** When the incident signals are all noncircular ones, the proposed method will be equivalent to the method in [26] except that the way to construct the new data vector  $\check{\mathbf{z}}$  is different.

**Remark 4:** It should be mentioned that the number of columns of  $\mathbf{E}_n$  should be no less than 4. Therefore,  $4M - K_n - 2K_c \geq 4$  must be satisfied to use (23) and (24). For  $M$  elements in each ULA, Xia's method in [3] can detect  $K_n$  noncircular and  $K_c$  circular signals up to  $K_n + K_c = 2(M - 1)$ , while our proposed method can estimate  $2K_n$  noncircular signals for the same  $K_c$  of circular signals and therefore, the total number of incident signals is  $K_n + 2K_c = 4(M - 1)$ ; Liu's method in [26] can only distinguish  $4(M - 1)$  noncircular signals.

**Remark 5:** In contrast to existing methods, the proposed one has three main advantages. Firstly, it can perform a more accurate estimation in situations where the number of sources is within the traditional limit of high resolution methods; secondly, it can still work effectively when the number of mixed signals is larger than that of the sensor elements; thirdly, the proposed method has a much lower computational complexity to achieve the automatically paired 2-D DOAs without the complicated 2-D spectrum peak search. As with other DOA estimation algorithms, when angle separation of the impinging signals is small, it will suffer from a high RMSE value and its performance will improve with a larger separation angle, as demonstrated in Subsection IV.D. Moreover, although 2-D spectrum search can be avoided with the proposed algorithm, its computational complexity is still high and further reduction is needed in the future.

**Remark 6:** It should be pointed out that the conclusion about the additional number of source signals which can be resolved by the proposed algorithm is only valid in the presence of strictly noncircular signals. However, the proposed algorithm is also applicable to arbitrary non-circular signals with at least one strictly noncircular signal. In this case the algorithm will treat the arbitrary noncircular signals (excluding the strictly non-circular one) in the same way as the circular signals. When there is no strictly non-circular signals, i.e.  $K_n = 0$ , we can directly use (27) or (39) and (40) to estimate the directions of arbitrary non-circular signals or a mixture of both circular and arbitrary non-circular signals. One note is, in theory, although we will be able to achieve an improved

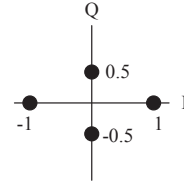


Fig. 2. The I/Q diagram of a UQPSK signal with a noncircularity coefficient 0.6.

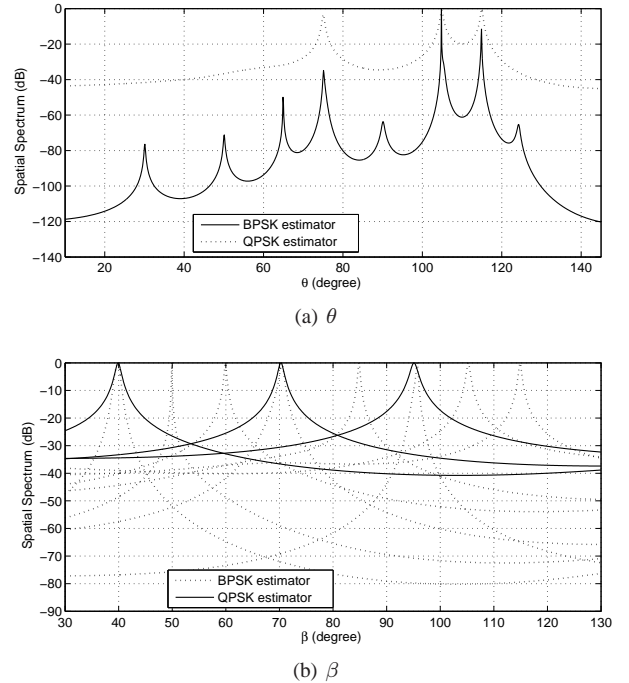


Fig. 3. Spatial spectrum of the estimators for BPSK and QPSK signals with SNR fixed at 20dB and the number of snapshots being 1500.

performance compared to the traditional ones due to the additional second order statistics information being exploited in the formulation, the improvement will not be observable for relatively high signal-to-noise ratio (SNR) scenarios (no strictly noncircular signals present), as already pointed out in [18]. One example for such arbitrary non-circular signals is the unbalanced quadrature phase shifting keying (UQPSK) signal whose complex components in the I/Q diagram have different powers, as shown in Fig.2 with a noncircularity coefficient of 0.6. In the next section, we will provide a simulation with a mixture of BPSK, UQPSK and QPSK signals.

#### IV. SIMULATION RESULTS

In this section, simulations are performed to illustrate the performance of the proposed algorithm. For all simulations, each of the two parallel ULAs has four elements except for the simulations A.2, D and E, which have five elements. Both  $d_x$  and  $d_y$  are half wavelength.

The mixed circular and non-circular incoming signals have equal power. The power of additive white Gaussian noise is  $\sigma_n^2$ . The SNR is defined as  $\text{SNR} = 10\log_{10}(\sigma_s^2/\sigma_n^2)$ . We use root mean square error (RMSE) to evaluate the

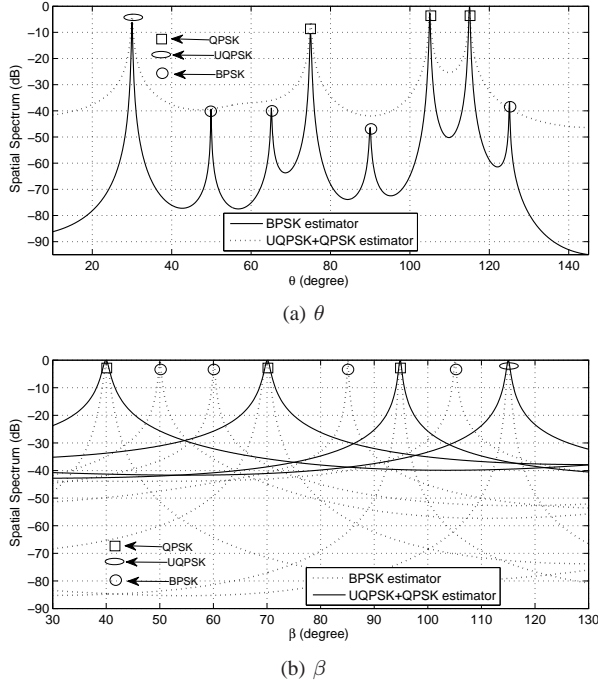


Fig. 4. Spatial spectrum of the estimators for BPSK, UQPSK and QPSK signals with SNR fixed at 20dB and the number of snapshots being 1500.

estimation performance, which is defined as  $RMSE = \sqrt{\frac{1}{K} \sum_{k=1}^K \sum_{q=1}^{M_c} [(\hat{\zeta}_{qk} - \zeta_k)^2]}$  where  $M_c = 100$  is the number of Monte Carlo simulations,  $K$  is the number of signals,  $\hat{\zeta}_{q,k}$  is the estimated result ( $\hat{\theta}_k$  or  $\hat{\beta}_k$ ) in the  $q$ th Monte Carlo simulation, and  $\zeta_k$  is the real value for either  $\theta_k$  or  $\beta_k$  of the  $k$ th signal. Besides, Xia's method in [3] and Liu's method in [26] are included for comparison.

#### A. Spatial spectrum of the estimators

1) *A mixture of BPSK and QPSK signals:* To demonstrate the resolution performance of the proposed method, we use five BPSK signals and three QPSK signals and in total there are eight signals. The BPSK signals are from directions  $(65^\circ, 50^\circ)$ ,  $(90^\circ, 105^\circ)$ ,  $(50^\circ, 60^\circ)$ ,  $(125^\circ, 85^\circ)$  and  $(30^\circ, 115^\circ)$ , while the QPSK signals from  $(105^\circ, 95^\circ)$ ,  $(75^\circ, 40^\circ)$  and  $(115^\circ, 70^\circ)$ . The SNR is 20dB. The number of snapshots is 1500. Fig. 3 (a) and (b) shows the spatial spectrum of the strictly noncircular and circular estimators related to  $\theta$  and  $\beta$  by the proposed algorithm, respectively, where the "BPSK estimator" uses equations (23) and (24), and the "QPSK estimator" uses equations (33) and (34). It can be seen that the eight signals are all distinguished successfully by the proposed algorithm where the condition  $K_n + 2K_c = 11 < 4(M - 1) = 12$  is met. For this case, both Xia's and Liu's methods have failed, because  $K_n + K_c = 8 > 2(M - 1) = 6$  with Xia's method, and for Liu's method, only BPSK signals can be estimated.

2) *A mixture of BPSK, UQPSK and QPSK signals:* In this set of simulations, we replace the BPSK signal from direction  $(30^\circ, 115^\circ)$  by a UQPSK one and increase the sensor

number to 5 with the other parameters the same as in the first simulation. The results in Fig. 4 (a) and (b) clearly show that the proposed method can still work with a mixture of BPSK, UQPSK and QPSK signals as discussed in **Remark 6**, where the "UQPSK+QPSK estimator" used equations (39) and (40).

#### B. Performance versus SNR

In this set of simulations, we study the performance with a varying SNR from 0dB to 30dB. There are four uncorrelated signals from directions  $(60^\circ, 50^\circ)$ ,  $(80^\circ, 70^\circ)$ ,  $(100^\circ, 85^\circ)$  and  $(125^\circ, 105^\circ)$ . We consider four cases where one, two, three and four BPSK signals are considered, respectively. The number of snapshots is 1200. As shown in Fig. 5 (a) and (b), the proposed method outperforms Xia's method in all cases because the noise subspace dimension increases by exploiting the conjugate information of the received data. Moreover, the 2-D DOA estimation performance of the proposed method improves from case 1 to case 4, and the reason for this is that the noise subspace has been extended by increasing the number of BPSK signals. Especially, for case 4 where the incoming signals are all BPSK, the proposed method is reduced to Liu's method except that the way to construct the new data vector  $\tilde{\mathbf{z}}$  is different. Therefore, in this case both methods have the same performance.

#### C. Performance versus number of snapshots

The performance of the proposed method is studied in this part with the number of snapshots varying from 50 to 750. The SNR is fixed at 15 dB and the other parameters are the same as in section B. The RMSE results for the three methods are shown in Fig. 6 (a) and (b), and we can draw similar conclusions as in section B.

#### D. Performance versus angle separation

Now the performance of the proposed method is investigated with the angle separation  $\Delta$  of 2-D DOAs varying from  $5^\circ$  to  $23^\circ$ . The SNR is fixed at 20dB and the snapshot number is 800. Four uncorrelated signals arrive from directions  $(65^\circ, 40^\circ)$ ,  $((65 + \Delta)^\circ, (40 + \Delta)^\circ)$ ,  $(100^\circ, 75^\circ)$  and  $((100 + \Delta)^\circ, (75 + \Delta)^\circ)$ . We consider three cases where one, two and three BPSK signals are present. Naturally, when angle separation is small, all methods will suffer with a high RMSE value and their performance will improve with a larger separation angle, as shown in Fig. 7 (a) and (b). Moreover, our proposed method again has outperformed Xia's method for all three cases.

#### E. Deterministic CRB [28] for strictly noncircular signals versus SNR

Here, we only study the deterministic CRB with case 4 mentioned in section B where all the incoming signals are BPSK. Keeping other parameters unchanged as in simulation B, we set the sensor number to five, and vary the SNR from -5dB to 20dB. As shown in Fig. 8 (a) and (b), the deterministic CRB for strictly noncircular signals denoted as  $CRB_{nc}$  has a lower RMSE value than the deterministic CRB for circular signals which is denoted as  $CRB_c$  at low SNRs which is in accordance to the analysis in [28].

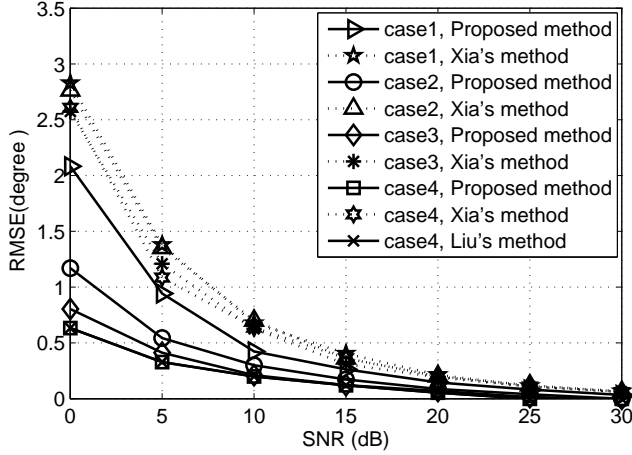
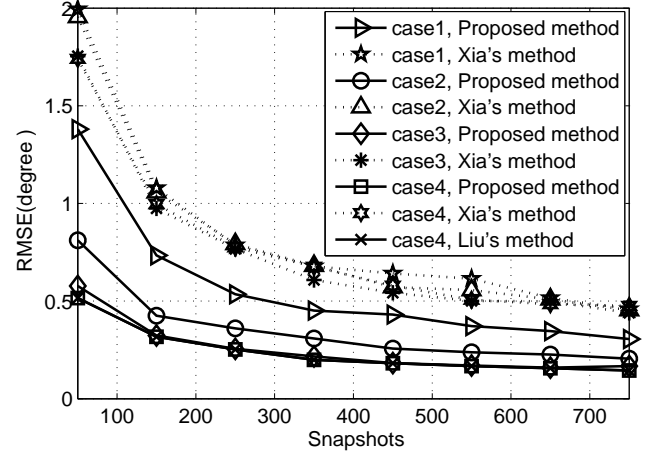
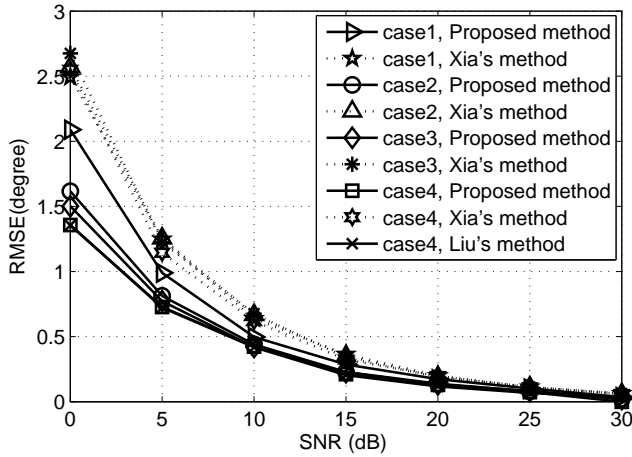
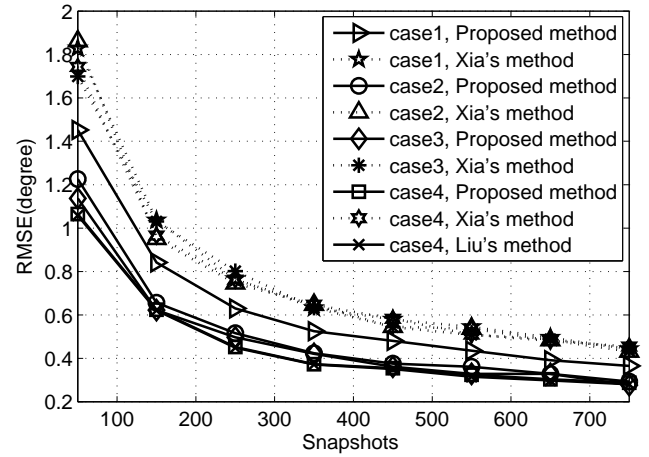
(a)  $\theta$ (a)  $\theta$ (b)  $\beta$ (b)  $\beta$ 

Fig. 5. RMSE of versus SNR with the snapshots being 1200.

Fig. 6. RMSE of versus snapshots with the SNR fixed at 15dB.

## V. CONCLUSION

A generalized 2-D DOA estimation algorithm for mixed circular and non-circular signals has been proposed based on a 2-D array structure consisting of two parallel ULAs. As also demonstrated by extensive simulation results, compared to existing methods, the proposed one has three main advantages. Firstly, it can give a more accurate estimation in situations where the number of sources is within the traditional limit of high resolution methods; secondly, it can still work effectively when the number of mixed signals is larger than that of the array elements; thirdly, the paired 2-D DOAs of the proposed method can be obtained automatically without the complicated 2-D spectrum peak search and therefore has a much lower computational complexity.

## APPENDIX

Here, we prove that (30) and (31) are equivalent.

*Proof:* The orthogonality between  $\mathbf{E}_n$  and  $\check{\mathbf{C}}$  can be expanded as

$$\begin{bmatrix} \mathbf{E}_{n1}^H & \mathbf{E}_{n2}^H \end{bmatrix} \begin{bmatrix} \mathbf{C}_1 & \mathbf{C}_2 & \mathbf{0}_{2M \times K_c} \\ \mathbf{C}_1^* & \mathbf{0}_{2M \times K_c} & \mathbf{C}_2^* \end{bmatrix} = \mathbf{0} \quad (41)$$

Due to  $\mathbf{E}_{n1}^H$ ,  $\mathbf{E}_{n2}^H$ ,  $\mathbf{C}_1$ ,  $\mathbf{C}_1^*$ ,  $\mathbf{C}_2$  and  $\mathbf{C}_2^*$  are block matrices, (41) can be rewritten in the following form

$$\begin{bmatrix} \mathbf{E}_{n2}^H & \mathbf{E}_{n1}^H \end{bmatrix} \begin{bmatrix} \mathbf{C}_1^* & \mathbf{C}_2^* & \mathbf{0}_{2M \times K_c} \\ \mathbf{C}_1 & \mathbf{0}_{2M \times K_c} & \mathbf{C}_2 \end{bmatrix} = \mathbf{0} \quad (42)$$

Applying the conjugate operation on both sides of (42), we obtain

$$\begin{bmatrix} \mathbf{E}_{n2}^T & \mathbf{E}_{n1}^T \end{bmatrix} \begin{bmatrix} \mathbf{C}_1 & \mathbf{C}_2 & \mathbf{0}_{2M \times K_c} \\ \mathbf{C}_1^* & \mathbf{0}_{2M \times K_c} & \mathbf{C}_2^* \end{bmatrix} = \mathbf{0} \quad (43)$$

Define  $\tilde{\mathbf{E}}_n = \begin{bmatrix} \mathbf{E}_{n2}^T & \mathbf{E}_{n1}^T \end{bmatrix}^H$  which is an orthonormal matrix. Then (43) can be rewritten as

$$\tilde{\mathbf{E}}_n^H \check{\mathbf{C}} = \mathbf{0} \quad (44)$$

Since  $\check{\mathbf{C}}$  is a full-column-rank matrix,  $\tilde{\mathbf{E}}_n$  will also span the noise subspace. From the uniqueness of the projection matrix onto a subspace, one can readily conclude that

$$\mathbf{P} = \mathbf{E}_n \mathbf{E}_n^H = \tilde{\mathbf{E}}_n \tilde{\mathbf{E}}_n^H \quad (45)$$

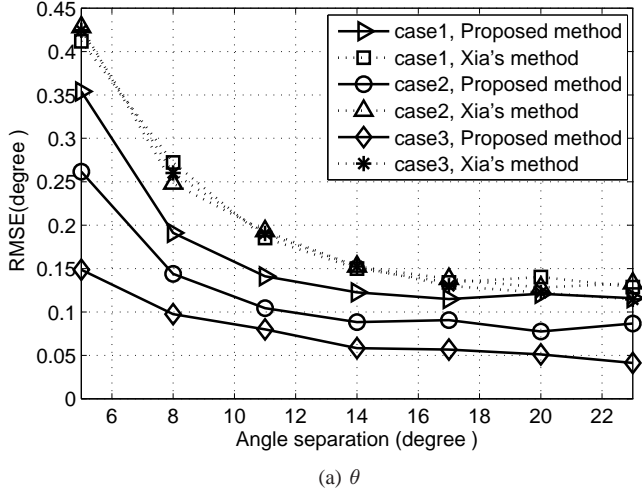
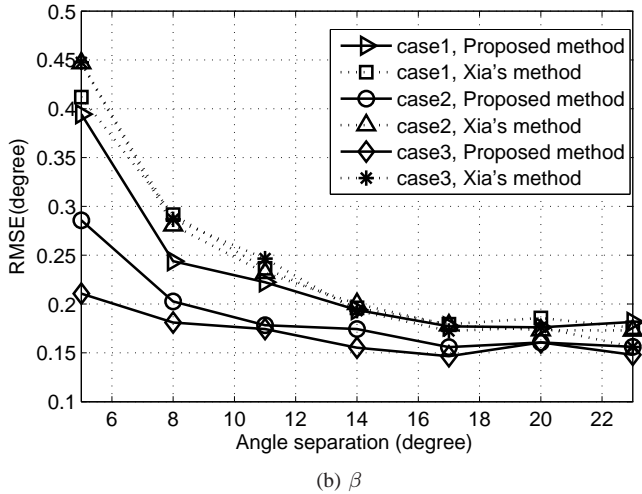
(a)  $\theta$ (b)  $\beta$ 

Fig. 7. RMSE versus angle separation with with SNR fixed at 20dB and the number of snapshots being 800.

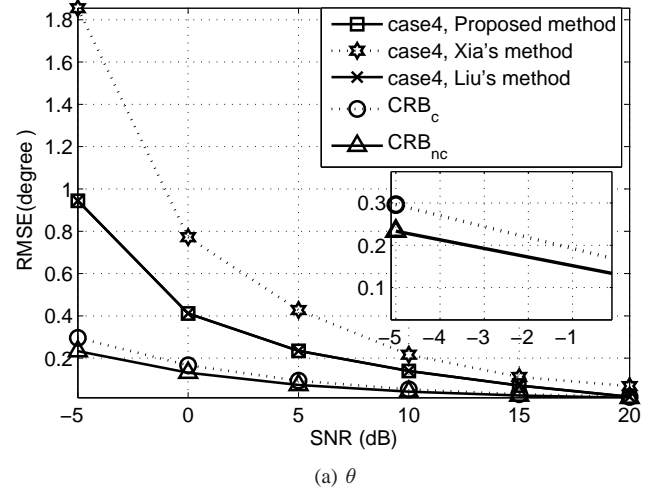
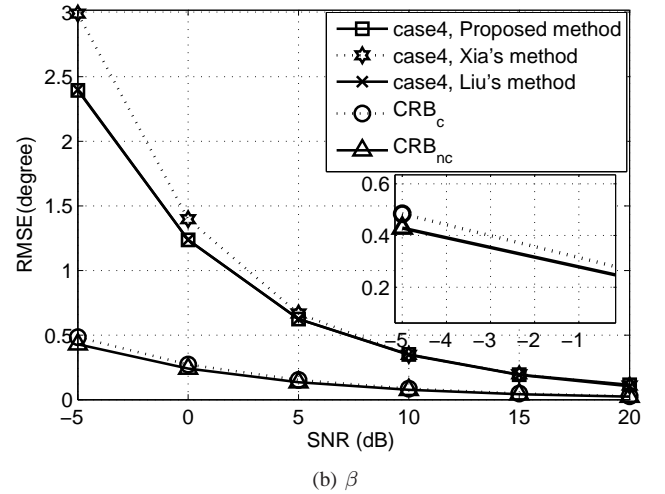
(a)  $\theta$ (b)  $\beta$ 

Fig. 8. RMSE of CRB versus SNR with the snapshots being 1200.

where

$$\begin{aligned} \mathbf{E}_n \mathbf{E}_n^H &= \begin{bmatrix} \mathbf{E}_{n1} \\ \mathbf{E}_{n2} \end{bmatrix} \begin{bmatrix} \mathbf{E}_{n1}^H & \mathbf{E}_{n2}^H \end{bmatrix} \\ &= \begin{bmatrix} \mathbf{E}_{n1} \mathbf{E}_{n1}^H & \mathbf{E}_{n1} \mathbf{E}_{n2}^H \\ \mathbf{E}_{n2} \mathbf{E}_{n1}^H & \mathbf{E}_{n2} \mathbf{E}_{n2}^H \end{bmatrix} \end{aligned} \quad (46)$$

$$\begin{aligned} \tilde{\mathbf{E}}_n \tilde{\mathbf{E}}_n^H &= \begin{bmatrix} \tilde{\mathbf{E}}_{n2}^* \\ \tilde{\mathbf{E}}_{n1}^* \end{bmatrix} \begin{bmatrix} \tilde{\mathbf{E}}_{n2}^T & \tilde{\mathbf{E}}_{n1}^T \end{bmatrix} \\ &= \begin{bmatrix} \tilde{\mathbf{E}}_{n2}^* \tilde{\mathbf{E}}_{n2}^T & \tilde{\mathbf{E}}_{n2}^* \tilde{\mathbf{E}}_{n1}^T \\ \tilde{\mathbf{E}}_{n1}^* \tilde{\mathbf{E}}_{n2}^T & \tilde{\mathbf{E}}_{n1}^* \tilde{\mathbf{E}}_{n1}^T \end{bmatrix} \\ &= \begin{bmatrix} (\tilde{\mathbf{E}}_{n2} \tilde{\mathbf{E}}_{n2}^H)^* & (\tilde{\mathbf{E}}_{n2} \tilde{\mathbf{E}}_{n1}^H)^* \\ (\tilde{\mathbf{E}}_{n1} \tilde{\mathbf{E}}_{n2}^H)^* & (\tilde{\mathbf{E}}_{n1} \tilde{\mathbf{E}}_{n1}^H)^* \end{bmatrix} \end{aligned} \quad (47)$$

Therefore, we have the following equation

$$\mathbf{E}_{n1} \mathbf{E}_{n1}^H = (\mathbf{E}_{n2} \mathbf{E}_{n2}^H)^*, \quad (48)$$

which completes the proof.

#### REFERENCES

- [1] H. Krim and M. Viberg, "Two decades of array signal processing research: the parametric approach," *IEEE Signal Processing Magazine*, vol. 13, no. 4, pp. 67–94, 1996.
- [2] J. Liang, "Joint azimuth and elevation direction finding using cumulant," *IEEE Sensors Journal*, vol. 9, no. 4, pp. 390–398, 2009.
- [3] T. Xia, Y. Zheng, Q. Wan, and X. Wang, "Decoupled estimation of 2-D angles of arrival using two parallel uniform linear arrays," *IEEE Transactions on Antennas and Propagation*, vol. 55, no. 9, pp. 2627–2632, 2007.
- [4] Q.-Y. Yin, R. Newcomb, and L.-H. Zou, "Estimating 2-D angles of arrival via two parallel linear arrays," in *Acoustics, Speech, and Signal Processing, 1989. ICASSP-89., 1989 International Conference on*. IEEE, 1989, pp. 2803–2806.
- [5] H. Tao, J. Xin, J. Wang, N. Zheng, and A. Sano, "Two-dimensional direction estimation for a mixture of noncoherent and coherent signals," *IEEE Transactions on Signal Processing*, vol. 63, no. 2, pp. 318–333, 2015.
- [6] H. Chen, C.-P. Hou, Q. Wang, L. Huang, and W.-Q. Yan, "Cumulants-based toeplitz matrices reconstruction method for 2-D coherent DOA estimation," *IEEE Sensors Journal*, vol. 14, no. 8, pp. 2824–2832, 2014.
- [7] Y. Wu, G. Liao, and H.-C. So, "A fast algorithm for 2-D direction-of-arrival estimation," *Signal processing*, vol. 83, no. 8, pp. 1827–1831, 2003.
- [8] J. Liang and D. Liu, "Joint elevation and azimuth direction finding using L-shaped array," *IEEE Transactions on Antennas and Propagation*, vol. 58, no. 6, pp. 2136–2141, 2010.
- [9] G. Wang, J. Xin, N. Zheng, and A. Sano, "Computationally efficient subspace-based method for two-dimensional direction estimation with L-shaped array," *IEEE Transactions on Signal Processing*, vol. 59, no. 7, pp. 3197–3212, 2011.
- [10] N. Tayem and H. M. Kwon, "L-shape 2-dimensional arrival angle

- estimation with propagator method," *IEEE Transactions on Antennas and Propagation*, vol. 53, no. 5, pp. 1622–1630, 2005.
- [11] S. Kikuchi, H. Tsuji, and A. Sano, "Pair-matching method for estimating 2-D angle of arrival with a cross-correlation matrix," *IEEE Antennas and Wireless Propagation Letters*, vol. 5, no. 1, pp. 35–40, 2006.
  - [12] N. Xi and L. Liping, "A computationally efficient subspace algorithm for 2-D DOA estimation with L-shaped array," *IEEE Signal Processing Letters*, vol. 21, no. 8, pp. 971–974, 2014.
  - [13] J.-F. Gu and P. Wei, "Joint svd of two cross-correlation matrices to achieve automatic pairing in 2-D angle estimation problems," *IEEE Antennas and Wireless Propagation Letters*, vol. 6, pp. 553–556, 2007.
  - [14] Z. Ye and C. Liu, "2-D DOA estimation in the presence of mutual coupling," *IEEE Transactions on Antennas and Propagation*, vol. 56, no. 10, pp. 3150–3158, 2008.
  - [15] F.-J. Chen, S. Kwong, and C.-W. Kok, "Esprit-like two-dimensional DOA estimation for coherent signals," *IEEE Transactions on Aerospace and Electronic Systems*, vol. 46, no. 3, pp. 1477–1484, 2010.
  - [16] W. Zhang, W. Liu, J. Wang, and S. L. Wu, "Computationally efficient 2-D DOA estimation for uniform rectangular arrays," *Multidimensional Systems and Signal Processing*, vol. 25, pp. 847–857, October 2014.
  - [17] J. Liu, Z. Huang, and Y. Zhou, "Extended 2q-music algorithm for noncircular signals," *Signal Processing*, vol. 88, no. 6, pp. 1327–1339, 2008.
  - [18] J.-P. Delmas and H. Abeida, "Stochastic cramer-rao bound for noncircular signals with application to DOA estimation," *IEEE Transactions on Signal Processing*, vol. 52, no. 11, pp. 3192–3199, 2004.
  - [19] J. Steinwandt, F. Roemer, M. Haardt, and G. Del Galdo, "R-dimensional esprit-type algorithms for strictly second-order non-circular sources and their performance analysis," *IEEE Transactions on Signal Processing*, vol. 62, no. 18, pp. 4824–4838, 2014.
  - [20] H. Abeida and J.-P. Delmas, "Efficiency of subspace-based doa estimators," *Signal Processing*, vol. 87, no. 9, pp. 2075–2084, 2007.
  - [21] H. Abeida and J.-P. Delmas, "Music-like estimation of direction of arrival for noncircular sources," *IEEE Transactions on Signal Processing*, vol. 54, no. 7, pp. 2678–2690, 2006.
  - [22] M. Haardt and F. Romer, "Enhancements of unitary esprit for non-circular sources," in *Acoustics, Speech, and Signal Processing, 2004. Proceedings.(ICASSP'04). IEEE International Conference on*, vol. 2. IEEE, 2004, pp. ii–101.
  - [23] Z. Huang, Z. Liu, J. Liu, and Y. Zhou, "Performance analysis of music for non-circular signals in the presence of mutual coupling," *IET radar, sonar & navigation*, vol. 4, no. 5, pp. 703–711, 2010.
  - [24] P. Chargé, Y. Wang, and J. Saillard, "A non-circular sources direction finding method using polynomial rooting," *Signal Processing*, vol. 81, no. 8, pp. 1765–1770, 2001.
  - [25] H. Abeida and J.-P. Delmas, "Gaussian cramer-rao bound for direction estimation of noncircular signals in unknown noise fields," *IEEE Transactions on Signal Processing*, vol. 53, no. 12, pp. 4610–4618, 2005.
  - [26] J. Liu, Z. Huang, and Y. Zhou, "Azimuth and elevation estimation for noncircular signals," *Electronics letters*, vol. 43, no. 20, pp. 1117–1119, 2007.
  - [27] L. Gan, J.-F. Gu, and P. Wei, "Estimation of 2-D DOA for noncircular sources using simultaneous svd technique," *IEEE Antennas and Wireless Propagation Letters*, vol. 7, pp. 385–388, 2008.
  - [28] F. Roemer and M. Haardt, "Efficient 1-D and 2-D DOA estimation for non-circular sources with hexagonal shaped espar arrays," in *Acoustics, Speech and Signal Processing, 2006. ICASSP 2006 Proceedings. 2006 IEEE International Conference on*, vol. 4. IEEE, 2006, pp. IV–IV.
  - [29] F. Gao, A. Nallanathan, and Y. Wang, "Improved music under the coexistence of both circular and noncircular sources," *IEEE Transactions on Signal Processing*, vol. 56, no. 7, pp. 3033–3038, 2008.
  - [30] A. Liu, G. Liao, Q. Xu, and C. Zeng, "A circularity-based DOA estimation method under coexistence of noncircular and circular signals," in *Acoustics, Speech and Signal Processing (ICASSP), 2012 IEEE International Conference on*. IEEE, 2012, pp. 2561–2564.
  - [31] Z.-M. Liu, Z.-T. Huang, Y.-Y. Zhou, and J. Liu, "Direction-of-arrival estimation of noncircular signals via sparse representation," *IEEE Transactions on Aerospace and Electronic Systems*, vol. 48, no. 3, pp. 2690–2698, 2012.
  - [32] P. J. Schreier, "Bounds on the degree of impropriety of complex random vectors," *IEEE Signal Processing Letters*, vol. 15, pp. 190–193, 2008.
  - [33] J. P. Delmas and H. Abeida, "Asymptotic distribution of circularity coefficients estimate of complex random variables," *Signal Processing*, vol. 89, no. 12, pp. 2670–2675, 2009.